Received 21 November 2017; revised 2 January 2018; accepted 27 January 2018. Date of publication 31 January 2018; date of current version 23 February 2018. The review of this paper was arranged by Editor A. G. U. Perera.

Digital Object Identifier 10.1109/JEDS.2018.2800049

Analysis and Simulation of Low-Frequency Noise in Indium-Zinc-Oxide Thin-Film Transistors

YUAN LIU [1,2] (Member, IEEE), HONGYU HE [3] (Member, IEEE), RONGSHENG CHEN [1] (Member, IEEE), YUN-FEI EN [2] (Member, IEEE), BIN LI [2] (Member, IEEE), AND YI-QIANG CHEN [2] (Member, IEEE)

1 School of Microelectronics, South China University of Technology, Guangzhou 510640, China
2 Science and Technology on Reliability Physics and Application of Electronic Component Laboratory, CEPREI, Guangzhou 510610, China
3 School of Electrical Engineering, University of South China, Hengyang 421001, China

CORRESPONDING AUTHORS: R. CHEN and Y.-Q. CHEN (e-mail: rschen@connect.ust.hk; yiqiang-chen@hotmail.com)

This work was supported in part by the National Natural Science Foundation of China under Grant 61574048 and Grant 61604057, in part by the Science and Technology Research Project of Guangdong under Grant 2015B090912002 and Grant 2016A030310360, and in part by the Pearl River S&T Nova Program of Guangzhou under Grant 201710010172.

ABSTRACT Low-frequency noise (LFN) is investigated in a set of indium-zinc-oxide thin-film transistors (IZO TFTs) with fixed channel width ($W = 10\ \mu$m) and different channel lengths ($L = 10$, 20, 30, and 40 μm) from sub-threshold, linear to saturation regions. The drain current noise power spectral density is measured as a function of effective gate voltage and drain current. The variation slopes of normalized noise with effective gate voltage are in the range of -1.27 and -1.48, which are close to the prediction of the mobility fluctuation mechanism. According to the $\Delta N - \Delta\mu$ model, the flat-band voltage noise spectral density and Coulomb scattering coefficient are extracted. Subsequently, variations of noise with the drain current in the above threshold region are analyzed by considering the band-gap distribution of the tail states. Finally, the BSIM model is also used to model $1/f$ noise in the IZO TFTs. The noise parameter *NOIB* is extracted which is inversely proportional to the effective gate voltage. Good agreements are achieved between the simulated and measured results in the linear region.

INDEX TERMS Indium-zinc-oxide, thin film transistor, low frequency noise, BSIM.

I. INTRODUCTION

With high electrical performance and high optical transparency, indium-zinc-oxide thin-film transistors (IZO TFTs) have drawn great attention in ultra high definition displays [1]. For both display and image capture applications, IZO TFTs act as switching components for addressing the pixel circuit [2], [3]. Moreover, IZO TFT can also be integrated as peripheral drive circuits on glass substrates with low production costs [4].

The noise behavior of semiconductor devices is a key parameter in the analog circuit applications [5] and it sets the lower limit of the signal level which can be detected and processed by subsequent circuits and systems [6]. The noise performances are primarily dominated by thermal noise and flicker noise (1/f noise) [6], [7]. Thermal noise is mainly caused by the channel resistance while flicker noise appears through both quality dependent and fundamental noise processes [6]. Attributed to localized traps in the channel and border traps in the gate oxide, the noise levels in IZO TFTs are higher than those observed in crystalline silicon (c-Si) MOSFETs [8]–[11]. Such a high noise level may limit the use of IZO TFTs and should therefore be carefully studied and minimized.

Generally, there are two major existing theories to explain the origin of low frequency noise (LFN) [12]–[14]. The carrier number fluctuation mechanism states that flicker noise is attributed to the trapping and emission processes of charges in the border traps near the gate insulator/channel interface. On the other hand, the bulk mobility fluctuation mechanism considers that flicker noise is a result of the fluctuation in bulk mobility, which is induced by fluctuations in phonon population through scattering. Recently, flicker noise in IZO TFTs has been reported and the dominant mechanism has been discussed by many groups [8], [15]–[17].

In the design process of peripheral drive circuits, simulation and analysis of noise behaviors are very important. The LFN may up-convert to high frequencies which is a

2168-6734 © 2018 IEEE. Translations and content mining are permitted for academic research only.
Personal use is also permitted, but republication/redistribution requires IEEE permission.
See http://www.ieee.org/publications_standards/publications/rights/index.html for more information.

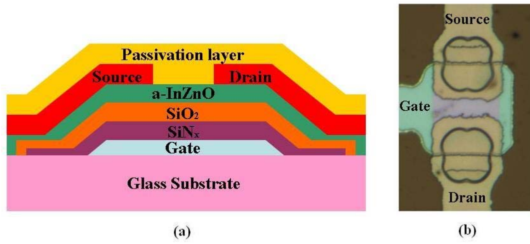

FIGURE 1. (a) Cross-section view and (b) plane view photograph of an IZO TFT with an inverted staggered bottom gate structure.

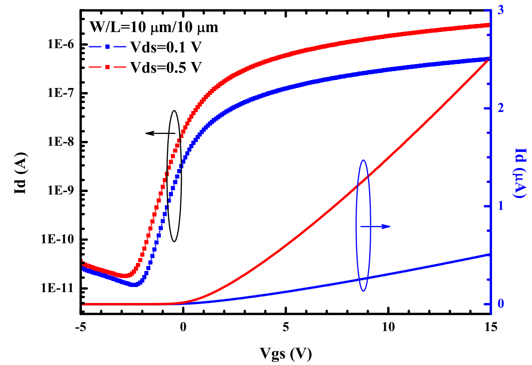

FIGURE 2. Transfer characteristics in the indium-zinc-oxide TFTs. Left axis: drain current with log scale. Right axis: drain current with linear scale.

dominant contributor to phase noise, thus adversely affecting the operation of IZO TFTs in analog and RF applications [5]. In order to evaluate the noise performance of the whole circuit, the designer uses one of the noise models available in the simulators [6], [18]. For c-Si MOSFETs, the industry-standard Berkeley short-channel IGFET compact model (BSIM) has been widely used to describe the 1/f noise from sub-threshold to strong inversion [19]–[21]. By extracting three fitting parameters (*NOIA*, *NOIB* and *NOIC*), the flicker noise can be simulated by this unified model in all operation regions. For amorphous silicon TFTs, Rigaud *et al.* [22] presents some good noise simulation results by using BSIM3 model. However, the suitability of the BSIM noise model on IZO TFTs has not yet been examined.

In this paper, the flicker noise of IZO TFTs is analyzed and simulated in all operating regions. Firstly, noises are measured from the sub-threshold region to the saturation region with a frequency bandwidth from 1 Hz to 100k Hz. The dominant mechanisms of flicker noise in each region are subsequently discussed. In order to examine the suitability of the BSIM noise model on the IZO TFTs, noise parameter *NOIB* is extracted. Finally, the measured results of flicker noise are compared to the simulated results in the linear region.

II. DEVICE STRUCTURE AND I-V CHARACTERISTICS

The devices used in this work are IZO TFTs with a back channel etch (BCE) architecture. The cross-section and plane photograph of these devices are shown in Fig. 1. A bilayer SiO_2 (50 nm)-SiN_x (250 nm) film is used as the gate insulator, and a 30-nm-thick IZO film is used as the active layer. The channel width (W) is 10 μm and the channel lengths (L) are varied from 10 μm to 40 μm.

The I-V characteristics are measured by use of an Agilent B1500 and Cascade probe station (Summit 12000). The flicker noises are measured by use of a Keysight E4727A LFN analyzer, which includes a dynamic signal analyzer, filters and amplifiers.

The typical transfer characteristics with log and linear scales are plotted in Fig. 2. The extracted electrical parameters performed at $V_{ds} = 0.1$ V are summarized in Table 1.

TABLE 1. Extracted electrical parameters in indium-zinc-oxide TFTs.

W (μm)	10			
L (μm)	10	20	30	40
V_{th} (V)	1.7	2.1	2.0	2.5
μ (cm^2/Vs)	21.15	20.60	21.59	20.05
SS (V/dec)	0.776	0.654	0.839	0.811

III. MEASURED LOW FREQUENCY NOISE

A. ORIGIN OF LOW FREQUENCY NOISE

The typical low frequency noise characteristics in the IZO TFTs with W/L=10μm/10μm are plotted in Fig. 3. As Fig. 3 shows, the drain current noise power spectral densities (S_I) follow a $1/f^{\gamma}$ law, and γ are about 0.6∼0.7 when the frequency is below 3 kHz. This phenomenon suggests the flicker noise is the main noise source under low frequency conditions, and it is induced by fluctuations of the interfacial trapped charges [23], [24]. As reported [25], the deviation from 1 of γ illustrates that the vertical distribution of oxide trap density is nonuniform in the gate oxide. $\gamma < 1$ is expected when the oxide trap density is higher close to the SiO_2/IZO interface than that in the interior of the gate oxide. In addition, this phenomenon ($\gamma < 1$) is also related to the characteristic temperature of the localized states which exist in the channel.

Moreover, the measured drain current noises follow a $1/f^2$ law when the frequency is above 3 kHz, which suggests the generation-recombination (G-R) noise is the main noise source in the frequency range of 3 kHz and 100 kHz. As reported in [11] and [17], the G-R noise from the traps with different time constants can be added, and thus the superposition of many Lorentzians may result in the total spectrum with $1/f^{\gamma}$ dependence over several decades of frequency. The observed $1/f^2$ noises in this work are consistent with the above mechanism, which suggests the G-R induced fluctuation of the carrier density may also be the origin of the $1/f^{\gamma}$ noise.

B. DOMINANT MECHANISM OF FLICKER NOISE

There are two different mechanisms used for the analysis of flicker noise: carrier number fluctuation (ΔN) theory and

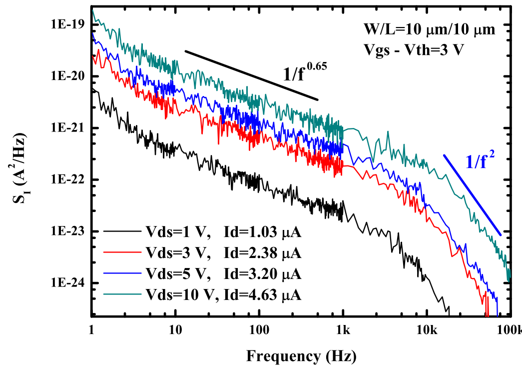

FIGURE 3. Drain current noise power spectral densities (S_I) for an IZO TFT with W/L= $10\mu m/10\mu m$, which are measured at different drain voltages (V_{ds}) from 1 V to 10 V and a constant effective gate voltage ($V_{gs} - V_{th}$) of 3 V.

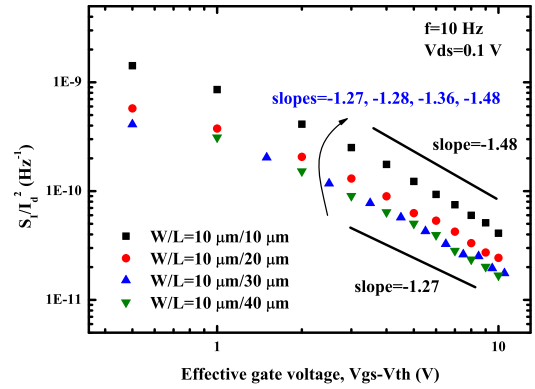

FIGURE 4. Normalized drain current noise (S_I/I_d^2) versus effective gate voltage for IZO TFTs with different channel length ($V_{ds} = 0.1$ V, $f = 10$ Hz).

mobility fluctuation ($\Delta\mu$) theory. In the classic carrier number fluctuation theory, the fluctuations in the drain current arise from the fluctuations of the interfacial charges due to the trapping and emission processes of free carriers into border traps and localized states. Thus, the normalized current noises (S_I/I_d^2) can be expressed by [8]

$$\frac{S_I}{I_d^2} = \frac{k^*}{f^\gamma C_{ox}^2 WL\left(V_{gs} - V_{th}\right)^2} \tag{1}$$

where C_{ox} is the gate insulator capacitance per unit area, and k^* is a fitting parameter that is related to the tunneling possibility between the channel and border traps.

In contrast to carrier number fluctuation theory, Hooge claimed the 1/f noise may originate from noise in lattice scattering, which in turn causes random mobility fluctuation [8], [14]. According to Hooge's empirical model, the normalized current noise can be expressed by [8], [14]

$$\frac{S_I}{I_d^2} = \frac{\alpha_H}{N_{tot} f^\gamma} = \frac{\alpha_H q}{f^\gamma C_{ox} WL\left(V_{gs} - V_{th}\right)} \tag{2}$$

where α_H is Hooge's empirical parameter which is technology and material dependent. N_{tot} is the total number of free charge carriers in the channel. The Hooge's empirical model is not only derived for homogeneous semiconductor devices, but also being widely used in the analysis of various TFT technologies (a-Si:H TFTs, IGZO TFTs and organic TFTs) [8].

To examine the dominant mechanism of flicker noise in the IZO TFTs, the dependence of normalized drain current noise on effective gate voltage ($V_{gs} - V_{th}$) is plotted in Fig. 4, as measured at drain voltage $V_{ds} = 0.1$ V and frequency f = 10 Hz in the IZO TFTs. Fig. 4 illustrates that the normalized noises have a power law dependence with $V_{gs} - V_{th}$ and the extracted power law coefficients are in the range of -1.27 and -1.48. Therefore, they are close to the prediction of the mobility fluctuation mechanism. Similar trends have also been observed in the a-Si:H TFTs [13] and IGZO TFTs [8], [9].

As plotted in Fig. 4, a reduction of the channel length leads to a modification of the law followed by S_I/I_d^2 against $V_{gs} - V_{th}$ from -1.27 to -1.48. These behaviors may relate to the modification of the origin of flicker noise [13]. The presence of bulk defects is more important in long channel amorphous thin film transistors, and it may push the bulk effect noise to be the predominant origin of the whole noise. As the decrement of channel length, the quality of the oxide/channel interface is critical, and the carrier number fluctuation induced by trapping/detrapping of free carriers in the localized states and/or border traps becomes more important [13]. Thus, IZO TFTs may varied from bulk dominated devices to interface dominated devices with the decrement of channel length. This finding may result in a shift of the power law coefficient of S_I/I_d^2 against $V_{gs} - V_{th}$.

The effective mobility in IZO TFTs is strongly dependent on the free carriers in the channel. Therefore, the fluctuation of interfacial charges may lead to the variation of mobility. As reported [26], [27], if the effective mobility is explicitly dependent on the interfacial charges, an extra drain current fluctuation may be induced and the related noises can be modeled by the carrier number with correlated mobility fluctuations (ΔN-$\Delta\mu$) model [26], [27]

$$\frac{S_I}{I_d^2} = \left(1 \pm \alpha_c \mu_{eff} C_{ox} I_d / g_m\right)\left(\frac{g_m}{I_d}\right)^2 \cdot S_{vfb} \tag{3}$$

where g_m is the device transconductance, and α_c is a fitting parameter which may be related to the coulomb scattering. A high value of α_c means more sensitivity of the mobility to the insulator charge. For a pure ΔN model, $\alpha_c \approx 0$. μ_{eff} is the field effect mobility, and S_{vfb} is the flat-band voltage noise power spectral density which can be expressed by [17], [27]

$$S_{vfb} = \frac{q^2 KT\lambda N_t}{WLC_{ox}^2 f^\gamma} \tag{4}$$

where λ is the tunneling attenuation coefficient (0.1 nm for SiO_2) and N_t is the trap density near the insulator/channel interface ($cm^{-2}eV^{-1}$).

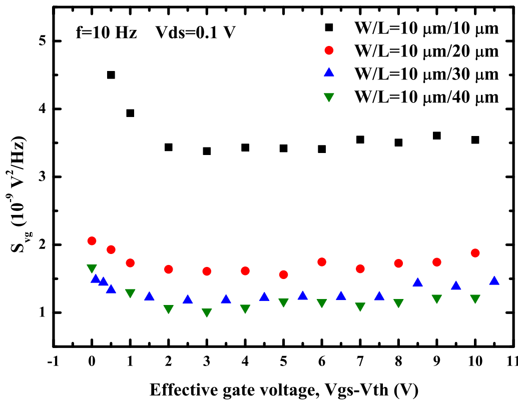

FIGURE 5. Variation of the gate voltage noise spectral density with the effective gate voltage in the IZO TFTs.

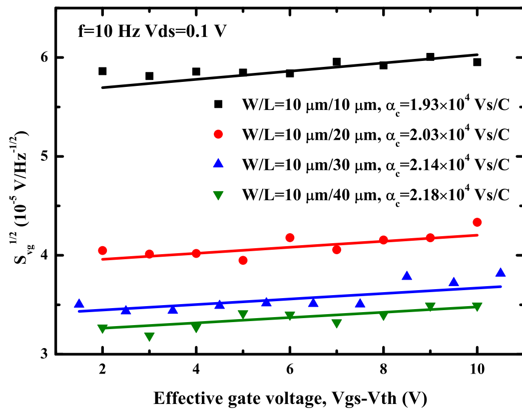

FIGURE 6. Variation of the root square gate voltage noise spectral density with the effective gate voltage in the IZO TFT. The solid lines are the best fits of the noise data.

Moreover, the gate voltage noise spectral density in the above threshold region is given by [26], [27]

$$S_{vg} = \frac{S_I}{g_m^2} = S_{vfb}\left[1 \pm \alpha_c \mu_{eff} C_{ox}\left(V_{gs} - V_{th}\right)\right]^2 \quad (5)$$

The variations of S_{vg} as a function of $V_{gs} - V_{th}$ are plotted in Fig. 5. Under high gate voltages, S_{vg} are varying superlinearly with gate voltage. In contrast, under low gate voltages or in the below threshold region, a steep decrease of S_{vg} with gate voltage is observed, caused by the exponential variation of free carriers with the gate voltage [26]. Moreover, the variation slope of S_{vg} with the gate voltage may be dependent on the channel length and channel width under low gate voltages. Thus, the variation rate may increase as the channel length is reduced [26]. Similar behaviors are also observed in MOSFETs [26] and a-Si:H TFTs [22].

To extract the scattering parameter α_c and flat-band voltage noise spectral density S_{vfb} for IZO TFTs, the variations of $S_{vg}^{1/2}$ with $V_{gs} - V_{th}$ are shown in Fig. 6. The parameters S_{vfb} deduced from the noise data are around 3.15×10^{-9} V^2/Hz (L = 10 μm), 1.52×10^{-9} V^2/Hz (L = 20 μm), 1.15×10^{-9} V^2/Hz (L = 30 μm), and 1.03×10^{-9} V^2/Hz (L = 40 μm), respectively. Moreover, the values of α_c are in

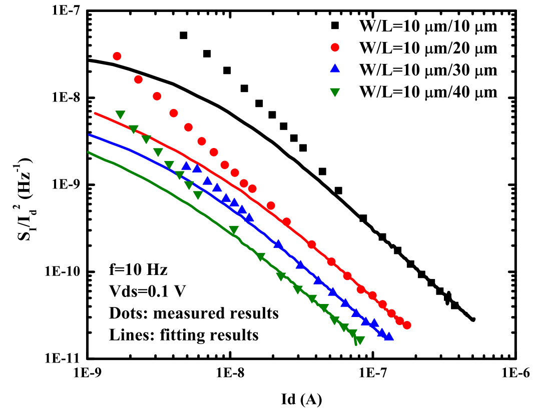

FIGURE 7. Normalized noise versus drain current in the ohmic region. The continuous lines are fit to (1) S_{vfb} = 3.15 × 10^{-9} V^2/Hz (L = 10 μm) (2) S_{vfb} = 1.52 × 10^{-9} V^2/Hz (L = 20 μm) (3) S_{vfb} = 1.15 × 10^{-9} V^2/Hz (L = 30 μm), and (4) S_{vfb} = 1.03 × 10^{-9} V^2/Hz (L = 40 μm).

the range of 1.93×10^4 and 2.18×10^4 Vs/C which decrease with the decrement of channel length. As discussed in the above section, the flicker noise in the short channel devices may be more affected by carrier number fluctuation, and thus results in the decrement of extracted α_c. Furthermore, as a comparison, the reported α_c is in the order of 10^4 Vs/C for c-Si MOSFETs [26], 8.7×10^5 Vs/C for IGZO TFTs [27], 1.5×10^4 Vs/C for Poly-Si TFTs [22] and 8.4×10^7 Vs/C for a-Si:H TFTs [28].

The normalized drain current noise versus drain current is shown in Fig. 7. By considering Eq. (3) associated with the interface charge fluctuations in the channel as in c-Si MOSFETs, the measured noises in the linear region are in good agreement with the fitting results by use of the above extracted parameters. However, under low drain current intensities, discrepancies occur between measured results and fitting results. This phenomenon is also observed in the poly-Si TFTs [23], [31]. Similar to large grain poly-Si TFTs, the excess of the measured noise from the theoretical results predicted by Eq. (3) in the IZO TFTs may due to carrier capture/release processes in localized states [23], [31]. In order to model these excess noises, another component should be added in Eq. (3) by considering the existence and contribution of localized states.

Furthermore, the S/D contact resistance may play an important role both in I-V [29] and noise characteristics [30] of short channel IZO TFTs. Thus, the flicker noise under high current intensities may be affected by the contact resistance, and it should be modeled by considering both the channel and contact resistance.

C. DENSITY OF LOCALIZED STATES

To extract the density of localized states (DOS) in the bandgap, the surface potential of IZO TFTs should be firstly calculated. As reported in [32], Lee *et al.* proposed a method for the calculation of surface potential (φ_s) from the subthreshold current. The surface potential can be calculated

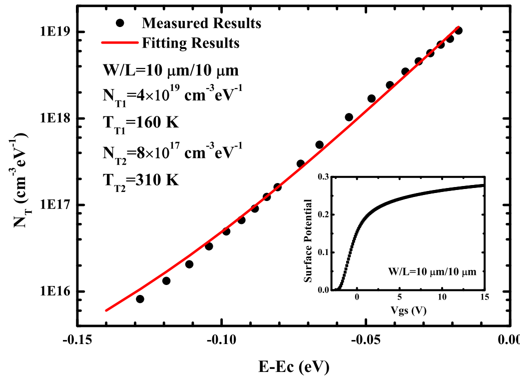

FIGURE 8. Calculated density of localized states in the band-gap from LFN characteristics. The insert figure is the surface potential calculated from the sub-threshold current for the IZO TFT.

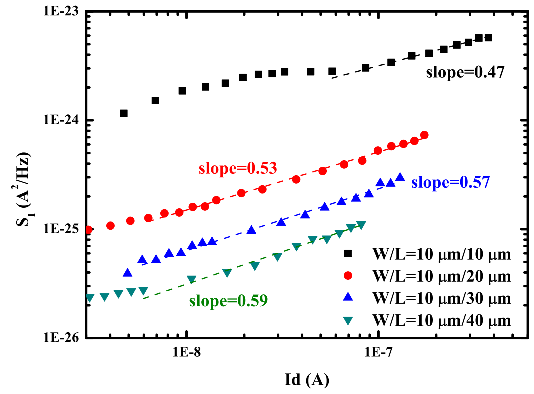

FIGURE 9. Variations of measured S_I (symbols) and corresponding simulation curves (solid lines) with drain current I_d in the linear region (Vds = 0.1V).

through nonlinear mapping of V_{gs} from the experimental sub-threshold current as

$$\varphi_s\left(V_{gs}\right) = \frac{1}{\Delta V_{gs}} \int V_T \ln\left(\frac{I_{D2}}{I_{D1}}\right) dV_g \tag{6}$$

where V_T is the thermal voltage, ΔV_{gs} is the measurement voltage step, and I_{D2} and I_{D1} are the measured current under two adjacent voltages. By using this method, the surface potential can be calculated, which is plotted in the insert figure of Fig. 8.

By considering traps within an energy band KT around the Fermi level, the corresponding density of localized states can be deduced by [33], [34]

$$N_T \approx \frac{4\lambda}{WLt_{ox}^2 KTf} \frac{I_d^2}{S_I} \tag{7}$$

Based on Eq. (6) and (7), the relation between DOS and subgap energy level can be extracted from the experimental I-V and noise characteristics, as plotted in Fig. 8.

The calculated $N_T(E)$ is consistent with the well-known distribution of DOS as a superposition of two exponential localized states which can be described by

$$N_T(E) = N_{T1} \cdot \exp\left(\frac{E-E_c}{KT_{T1}}\right) + N_{T2} \cdot \exp\left(\frac{E-E_c}{KT_{T2}}\right) \tag{8}$$

where N_{T1} and N_{T2} are about 4×10^{19} and 8×10^{17} $cm^{-3}eV^{-1}$, respectively. T_{T1} and T_{T2} are the characteristic temperatures of localized states which are about 160 K and 310 K, respectively.

Note here that extracted characteristic temperatures of localized states are close to the well-known characteristic temperatures of tail states [11], which are lower than that of deep states. To extract the density of deep states, the extraction method of φ_s should be improved and more LFN results should also be measured in the sub-threshold region.

IV. ANALYSIS OF FLICKER NOISE

A. NOISE IN THE ABOVE THRESHOLD REGION

Figure 9 shows drain current noise power spectral density versus drain current in the linear region at $V_{ds} = 0.1$ V. As shown in the Fig. 9, the noise S_I follows the power law dependence with I_d. The power law coefficients are extracted to be 0.47 to 0.59, which are lower than those observed in the c-Si MOSFETs (slope=1) [20]–[22]. These phenomena may induce by the existence of tail states in the channel [16].

As reported in [35] and [36], by considering tail states, the effective mobility is approximately given by

$$\mu_{eff} = \mu_0 \cdot \frac{Q_{free}}{Q_{tot}} \propto \left(V_{gs} - V_{th} - V_{ch}\right)^{\alpha} \tag{9}$$

where, Q_{free} and Q_{tot} is the density of the free carrier and the total induced charge in the channel, respectively. V_{ch} is the channel voltage and $\alpha = 2T_t/T - 2$, while T_t is the characteristic temperature of the tail states.

When V_{ds} is small, I_d in the linear region can be approximated by

$$\begin{aligned} I_d &= K_I\left[\left(V_{gs}-V_{th}\right)^{2+\alpha} - \left(V_{gs}-V_{th}-V_{ds}\right)^{2+\alpha}\right] \\ &\approx (2+\alpha)\, K_I\left(V_{gs}-V_{th}\right)^{1+\alpha} V_{ds} \end{aligned} \tag{10}$$

where, K_I is a modeling parameter that is related to the device structure and tail states.

Thus, g_m in the linear region can be calculated by

$$g_m = \frac{2+\alpha}{1+\alpha} K_I\left(V_{gs}-V_{th}\right)^{\alpha} V_{ds} \tag{11}$$

Substituting Eq. (10) and Eq. (11) into the first term of Eq. (3), the first term of Eq. (3) can be rewritten as [16]

$$\begin{aligned} S_I &= \left(\frac{2+\alpha}{1+\alpha}\right)^2 K_I^2\left(V_{gs}-V_{th}\right)^{2\alpha} V_{ds}^2 S_{vfb} \\ &= \frac{\left[(2+\alpha)\, K_I V_{ds}\right]^{2/(1+\alpha)}}{(1+\alpha)^2} S_{vfb} I_d^{2\alpha/(1+\alpha)} \\ &= \frac{C_{ox}^2\,(W/L)^2}{(1+\alpha)^2} V_{ds}^2 S_{vfb} \mu_{eff}^2 \end{aligned} \tag{12}$$

Based on Eq. (12), noise varied as $I_d^{2\alpha/(1+\alpha)}$ in the linear region. Combining with the power law coefficients (slopes) extracted from Fig. 9, α is calculated to be 0.31 to 0.42

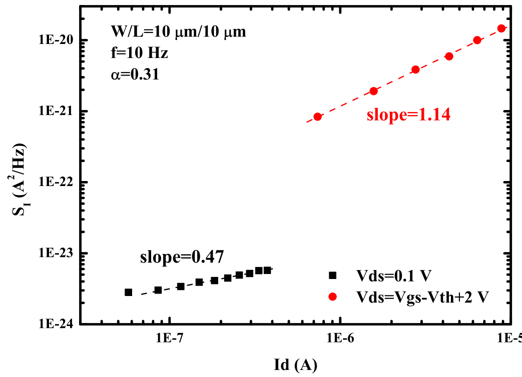

FIGURE 10. Variation of measured noise and simulation curves in the linear and saturation region.

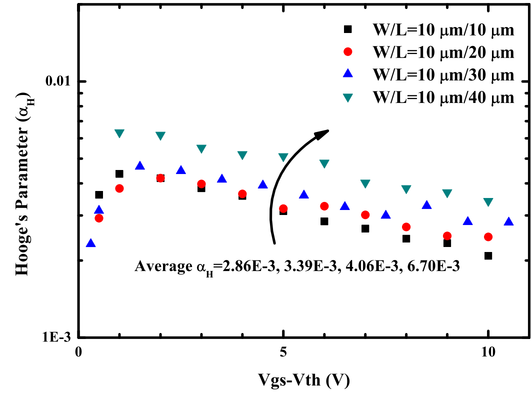

FIGURE 11. Extracted Hooge's parameters (α_H) versus $V_{gs} - V_{th}$ in the linear region for an IZO TFT with four channel lengths. (Vds = 0.1V).

in this paper. Thus, the related $T_t = (\alpha + 2)T/2$ is 345 K to 363 K in the IZO TFTs. These values are close to the extracted characteristic temperature of the tail states in the above section.

In the saturation region, $V_{dsat} = V_{gs} - V_{th}$, therefore noise can be expressed by [16]

$$S_I = \left(\frac{2+\alpha}{1+\alpha}\right)^2 K_I^2 \left(V_{gs} - V_{th}\right)^{2\alpha+2} S_{vfb} = \frac{\left[(2+\alpha) K_I V_{ds}\right]^{2/(2+\alpha)}}{(1+\alpha)^2} S_{vfb} I_d^{(2\alpha+2)/(2+\alpha)} \quad (13)$$

Based on Eq. (13), noise varied as $I_d^{(2\alpha+2)/(2+\alpha)}$ in the saturation region and the slope is lower than that in the c-Si MOSFETs which is equal to 1.5 [20]–[22]. As shown in Fig. 10, noise varies as $I_d^{1.14}$ and then the calculated α is nearly 0.31 which is consistent with the calculated values from the noise in the linear region.

In order to evaluate the quality of the channel material, α_H can be extracted from the measured noise data in the linear region. By rearranging Eq. (2), α_H can be calculated by

$$\alpha_H = \left(\frac{S_I}{I_d^2}\right) \frac{f^\gamma WLC_{ox}}{q} \left(V_{gs} - V_{th}\right) \quad (14)$$

As shown in Fig. 11, the extracted α_H decrease with the increase of effective gate voltage, which indicates the noise in the IZO TFTs may also be affected by the carrier number fluctuation mechanism. Note here that the inaccuracy of the extracted V_{th} may result in the increment of α_H under low effective gate voltages.

The values of average α_H are deduced to be about 2.86×10^{-3}, 3.39×10^{-3}, 4.06×10^{-3}, and 6.7×10^{-3} respectively. With the decrement of channel length, the flicker noise of IZO TFTs may be more affected by the quality of the IZO/SiO_2 interface than the bulk layer. In the above threshold region, most of the localized states near IZO/SiO_2 interface are filled with carriers while the bulk defects may be empty. Thus, the fluctuations induced by the localized states near IZO/SiO_2 interface may less than that induced by the bulk defect. It may leads to the decrement of α_H with the decrement of channel length.

α_H is frequently used as a device/material quality indicator, and it is usually lower in the higher quality electronic materials. As a comparison, α_H is about 5.32×10^{-3} in the mature a-Si:H TFTs and 1.35×10^{-3} in the IGZO TFTs [8], [22], [37]. Thus, our present result obtained for IZO TFTs shows good noise performance, which are in the same order to those reported mature TFTs [8], [22], [37].

B. NOISE IN THE SUB-THRESHOLD REGION

As shown in Fig. 7, the measured results in the sub-threshold clearly show that noise deviates from the theoretical results predicted by Eq. (3). These phenomena may induce by the existence of localized states (deep states) in the channel. In this region, extracted mobilities are not only related to lattice scattering, but also strongly dependent on the concentration of free carriers in the channel. Therefore, similar to Eq. (9), extracted effective mobility in the sub-threshold region also has a power dependence with $V_{gs} - V_{th}$ and the power law coefficient is a function of the characteristic temperature of deep states (T_d) in the channel [35], [36].

As reported [38], a simple empirical model can be used in the description of noise in the sub-threshold region for c-Si MOSFETs

$$\frac{S_I}{I_d^2} = \frac{\alpha_H}{N_{tot} f^\gamma} \cdot \left(\frac{\mu_{eff}}{\mu_0}\right)^2 \quad (15)$$

where μ_0 is the mobility which only affected by lattice scattering. The extracted S_I/I_d^2 versus measured μ_{eff} is plotted in Fig. 12. The slopes (M) are nearly -3 which is larger than the predicted result (slope= -2) by Eq. (15). Though the trend may be similar to the theoretical results predicted by Eq. (15), which are related to mobility fluctuation mechanism, the possible reason and the physical meaning of the parameter M are still unknown. However, they may relate to the distribution of deep states and we would like to discuss this in our future works.

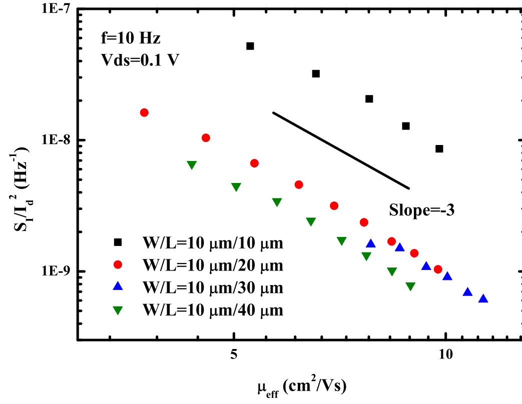

FIGURE 12. Extracted S_I/I_d^2 versus the effective mobility in the sub-threshold region.

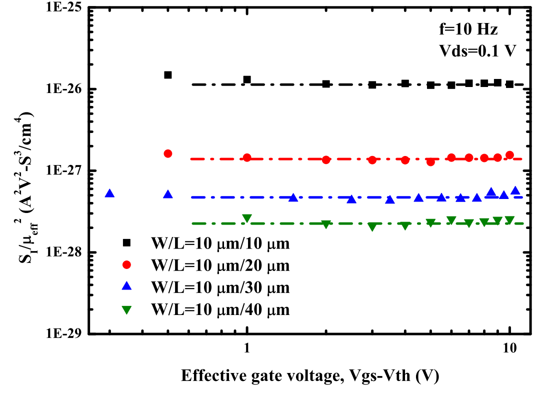

FIGURE 13. Typical evolutions of S_I/μ_{eff}^2 in the ohmic region, versus the effective gate voltage.

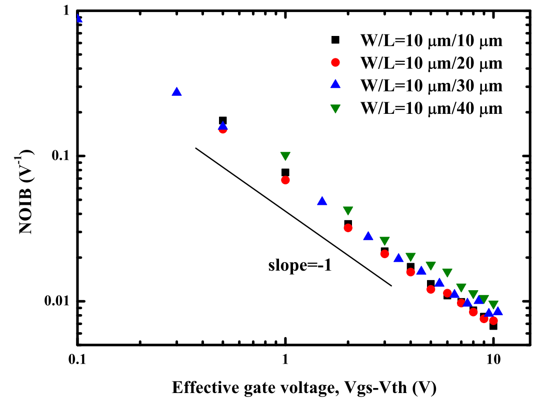

FIGURE 14. Extracted noise fitting parameter (*NOIB*) versus $V_{gs} - V_{th}$ in the above threshold region.

V. BSIM MODEL AND EXTRACTION RESULTS

In order to optimize the low frequency noise in analog applications, circuit designers may simulate noise performance by use of circuit simulators that take into account of the BSIM model. In this section, noise parameters used in the BSIM model are extracted for IZO TFTs.

The BSIM model provides two flicker models, the simple flicker model and the unified flicker model. In the unified model, Hung *et al.* [19] combine both carrier and related interface mobility fluctuation mechanisms. Thus, the flicker noise can be modeled by the use of three noise fitting parameters: *NOIA*, *NOIB* and *NOIC*.

In the sub-threshold region, by considering carrier number fluctuation theory, the noise is written as

$$S_{I,sub}(f) = \frac{NOIA}{N^{*2}} \frac{KTI_d^2}{W_{eff}L_{eff}f^{EF}(1/\lambda)} \tag{16}$$

where $NOIA = qN_t$ while N_t can be deduced by using Eq. (4) which are around 6.75×10^{17} cm^2eV^{-1} to 9.15×10^{17} cm^2eV^{-1} in this work, EF (flicker frequency exponent) characterizes the power dependence of the measured noise on frequency, and N^* can be calculated by

$$N^* = KT\left(C_{ox} + C_d + C_{it}\right)/q^2 \tag{17}$$

As discussed in the above sections, noise in the sub-threshold region may not only be affected by the carrier capture/release processes in traps located near the channel/insulator interface, but also affected by carrier capture/release processes in deep states in the channel. Thus, Eq. (16) is no longer suitable for the simulation in the IZO TFTs and it should be improved/modified by considering the existence of deep states.

In the above threshold region, the current noise is given by

$$S_{I,inv}(f) = \frac{KTq\mu_{eff}I_d}{C_{ox}L_{eff}^2f^{EF}}\begin{pmatrix} NOIA \cdot \log\left(\frac{N_0+N^*}{N_L+N^*}\right) \\ +NOIB \cdot (N_0 - N_L) \\ +NOIC \cdot (N_0^2 - N_L^2)/2 \end{pmatrix} + \frac{\Delta L_{clm}KTI_d^2}{qW_{eff}L_{eff}^2f^{EF}} \frac{NOIA + NOIB \cdot N_L + NOIC \cdot N_L^2}{(N_L + N^*)^2} \tag{18}$$

where ΔL_{clm} is a coefficient which is related to the channel length modulation effect. N_0 and N_L are the charge densities at the source and drain, which can be expressed by

$$qN_0 = C_{ox}\left(V_{gs} - V_{th}\right) \tag{19}$$

$$qN_L = C_{ox}\left(V_{gs} - V_{th} - \min\left(V_{ds}, V_{ds,sat}\right)\right) \tag{20}$$

For a small drain bias ($V_{ds} \ll V_{ds,sat}$ and $V_{ds} \ll V_{gs}$), by assuming $\Delta L_{clm} = 0$ and $NOIC = 0$, Eq. (18) can be further approximated by

$$S_{I,inv}(f) = \frac{KT\mu_{eff}I_d}{C_{ox}L_{eff}^2f^{EF}}V_{ds}C_{ox} \cdot NOIB = \frac{KT\mu_{eff}^2W_{eff}C_{ox}V_{ds}^2}{L_{eff}^3f^{EF}}\left(V_{gs} - V_{th}\right) \cdot NOIB \tag{21}$$

Combining Eq. (2) and Eq. (21), $NOIB = q\alpha_H/KT$. According to Eq. (12), S_I/μ_{eff}^2 is independent of $V_{gs} - V_{th}$ which is consistent with Mc Whorter's theory [20]. The values of S_I/μ_{eff}^2 at low drain biases versus $V_{gs} - V_{th}$ are plotted in Fig. 13. The extracted results agree well with the predicted results by Eq. (12).

If S_I/μ_{eff}^2 is independent of $V_{gs} - V_{th}$, the dependence of parameters *NOIB* on $(V_{gs} - V_{th})^{-1}$ is in accordance with Eq. (21). The *NOIB* parameters have been extracted, as shown in Fig. 14. The extracted results clearly show the

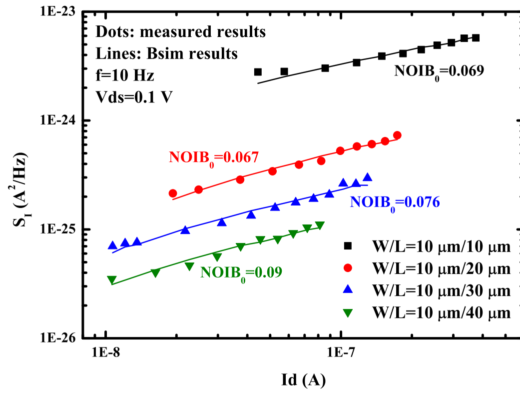

FIGURE 15. **Comparison between measured noise (dots) and BSIM simulated results (lines) in the linear region.**

slope is about −1 which is consistent with the predicted results. Therefore, *NOIB* can be further expressed by

$$NOIB = NOIB_0 \left(V_{gs} - V_{th}\right)^{-1} \tag{22}$$

In this work, the extracted $NOIB_0$ are constants which are about 0.069, 0.067, 0.076 and 0.09 for the IZO TFTs, respectively. Similar to α_H, the dependence of *NOIB* on channel length may also be induced by the variation of the dominant location of 1/f noise in IZO TFTs.

By use of Eq. (21) and Eq. (22), the simulated flicker noises in the linear region are plotted in Fig. 15. The simulated results agree well with the measured results in the linear region for the IZO TFTs.

VI. CONCLUSION

Low-frequency noises in the whole operation region of long channel IZO TFTs are investigated. The flicker noise is the main noise source when the frequency is below 3 kHz, while the generation-recombination noise is the dominant noise source in the frequency range from 3 kHz and 100 kHz. The measured results indicate that flicker noises are dominated by the mobility fluctuation mechanism and this can be explained by use of ΔN-$\Delta\mu$ fluctuation model. Moreover, the scaling-down of IZO TFTs may modify the dominant location of flicker noise. Thus, IZO TFTs may be varied from bulk dominated devices to interface dominated devices with the decrement of channel length, which results in the variation of extracted parameters α_H, α_c and *NOIB*. In addition, the density of localized states in the band-gap is extracted. The measured normalized noises are strongly dependent on the characteristic temperature of localized states in the channel. Finally, the suitability of the BSIM noise model on the IZO TFTs is examined. Good agreement is achieved between measured results and simulated results in the linear region.

REFERENCES

[1] H. Xu *et al.*, "High performance indium-zinc-oxide thin-film transistors fabricated with a back-channel-etch-technique," *Appl. Phys. Lett.*, vol. 99, no. 25, Dec. 2011, Art. no. 253501, doi: 10.1063/1.3670336.

[2] J. Y. Kwon *et al.*, "Bottom-gate gallium indium zinc oxide thin-film transistor array for high-resolution AMOLED display," *IEEE Electron Device Lett.*, vol. 29, no. 12, pp. 1309–1311, Dec. 2008, doi: 10.1109/LED.2008.2006637.

[3] C.-L. Lin, W.-Y. Chang, and C.-C. Hung, "Compensating pixel circuit driving AMOLED display with a-IGZO TFTs," *IEEE Electron Device Lett.*, vol. 34, no. 9, pp. 1166–1168, Sep. 2013, doi: 10.1109/LED.2013.2271783.

[4] M. Mativenga, M. H. Choi, J. W. Choi, and J. Jang, "Transparent flexible circuits based on amorphous indium–gallium–zinc–oxide thin film transistors," *IEEE Electron Device Lett.*, vol. 32, no. 2, pp. 170–172, Feb. 2011, doi: 10.1109/LED.2010.2093504.

[5] A. Jerng and C. G. Sodini, "The impact of device type and sizing on phase noise mechanisms," *IEEE J. Solid-State Circuits*, vol. 40, no. 2, pp. 360–369, Feb. 2005, doi: 10.1109/JSSC.2004.841035.

[6] T. Noulis, S. Siskos, and G. Sarrabayrouse, "Analysis and selection criteria of BSIM4 flicker noise simulation models," *Int. J. Circuit Theory Appl.*, vol. 36, no. 7, pp. 813–823, Oct. 2008, doi: 10.1002/cta.461.

[7] L. K. J. Vandamme, "Noise as a diagnostic tool for quality and reliability of electronic devices," *IEEE Trans. Electron Devices*, vol. 41, no. 11, pp. 2176–2187, Nov. 1994, doi: 10.1109/16.333839.

[8] T. C. Fung, G. Baek, and J. Kanicki, "Low frequency noise in long channel amorphous In-Ga-Zn-O thin film transistors," *J. Appl. Phys.*, vol. 108, no. 7, Oct. 2010, Art. no. 074518, doi: 10.1063/1.3490193.

[9] J.-M. Lee *et al.*, "Low-frequency noise in amorphous indium–gallium–zinc-oxide thin-film transistors," *IEEE Electron Device Lett.*, vol. 30, no. 5, pp. 505–507, May 2009, doi: 10.1109/LED.2009.2015783.

[10] C. Y. Jeong *et al.*, "Low-frequency noise properties in double-gate amorphous InGaZnO thin-film transistors fabricated by back-channel-etch method," *IEEE Electron Device Lett.*, vol. 36, no. 12, pp. 1332–1335, Dec. 2015, doi: 10.1109/LED.2015.2489223.

[11] S. Kim *et al.*, "Relation between low-frequency noise and subgap density of states in amorphous InGaZnO thin-film transistors," *IEEE Electron Device Lett.*, vol. 31, no. 11, pp. 1236–1238, Nov. 2010, doi: 10.1109/LED.2010.2061216.

[12] G. Ghibaudo and T. Boutchacha, "Electrical noise and RTS fluctuations in advanced CMOS devices," *Microelectron. Rel.*, vol. 42, nos. 4–5, pp. 573–582, Apr./May 2002, doi: 10.1016/S0026-2714(02)00025-2.

[13] J. Rhayem, M. Valenza, D. Riguad, M. Szydlo, and H. Lebrun, "1/f noise investigations in small channel length amorphous silicon thin film transistors," *J. Appl. Phys.*, vol. 83, no. 7, pp. 3660–3667, Apr. 1998, doi: 10.1063/1.366586.

[14] F. N. Hooge, "1/f noise sources," *IEEE Trans. Electron Devices*, vol. 41, no. 11, pp. 1926–1935, Nov. 1994, doi: 10.1109/16.333808.

[15] Y. Liu *et al.*, "Analysis of low-frequency noise in the amorphous indium zinc oxide thin film transistors," *Acta Physica Sinica*, vol. 63, no. 9, May 2014, Art. no. 098503, doi: 10.7498/aps.63.098503.

[16] H. He, X. R. Zheng, and S. D. Zhang, "1/f noise expressions for amorphous InGaZnO TFTs considering mobility power-law parameter in above-threshold regime," *IEEE Electron Device Lett.*, vol. 36, no. 2, pp. 156–158, Feb. 2015, doi: 10.1109/LED.2014.2378251.

[17] C. G. Theodorou *et al.*, "Origin of low-frequency noise in the low drain current range of bottom-gate amorphous IGZO thin-film transistors," *IEEE Electron Device Lett.*, vol. 32, no. 7, pp. 898–900, Jul. 2011, doi: 10.1109/LED.2011.2143386.

[18] T. Noulis, S. Siskos, and G. Sarrabayrouse, "Comparison between BSIM4.X and HSPICE flicker noise models in NMOS and PMOS transistors in all operating regions," *Microelectron. Rel.*, vol. 47, no. 8, pp. 1222–1227, Aug. 2008, doi: j.microrel.2006.09.021.

[19] K. K. Hung, P. K. Ko, C. Hu, and Y. C. Cheng, "A physics-based MOSFET noise model for circuit simulators," *IEEE Trans. Electron Devices*, vol. 37, no. 5, pp. 1323–1333, May 1990, doi: 10.1109/16.108195.

[20] J. C. Vildeuil, M. Valenza, and D. Rigaud, "Extraction of the BSIM3 1/f noise parameters in CMOS transistors," *Microelectron. J.*, vol. 30, no. 2, pp. 199–205, Feb. 1999, doi: 10.1016/S0026-2692(98)00108-6.

[21] Y. A. Allogo *et al.*, "1/f noise measurements in n-channel MOSFETs processed in 0.25 μm technology—Extraction of BSIM3v3 noise parameters," *Solid-State Electron.*, vol. 46, no. 3, pp. 361–366, Mar. 2002, doi: 10.1016/S0038-1101(01)00109-5.

[22] D. Riguad, M. Valenza, and J. Rhayem, "Low frequency noise in thin film transistors," *IET. Proc. Circuits Devices Syst.*, vol. 149, no. 1, pp. 75–82, Feb. 2002, doi: 10.1049/ip-cds:20020063.

[23] C. A. Dimitriadis, J. Brini, J. I. Lee, F. V. Farmakis, and G. Kamarinos, "1/f$^{\gamma}$ in polycrystalline silicon thin-film transistors," *J. Appl. Phys.*, vol. 85, no. 7, pp. 3934–3936, Apr. 1999, doi: 10.1063/1.369770.

[24] Y. Liu *et al.*, "Low-frequency noise characteristics in the MOSFETs processed in 65 nm technology," *J. Semicond.*, vol. 37, no. 6, Jun. 2016, Art. no. 064012, doi: 10.1088/1674-4926/37/6/064012.

[25] R. Jayaraman and C. G. Sodini, "A 1/f noise technique to extract the oxide trap density near the conduction band edge of silicon," *IEEE Trans. Electron Devices*, vol. 36, no. 9, pp. 1773–1782, Sep. 1989, doi: 10.1109/16.34242.

[26] G. Ghibaudo, O. Roux, C. Nguyen-Duc, F. Balestra, and J. Brini, "Improved analysis of low frequency noise in field-effect MOS transistors," *Phys. Status Solidi A*, vol. 124, no. 2, pp. 571–581, Apr. 1991, doi: 10.1002/pssa.2211240225.

[27] H.-S. Choi *et al.*, "Verification of interface state properties of a-InGaZnO thin-film transistors with SiNx and SiO2 gate dielectrics by low-frequency noise measurements," *IEEE Electron Device Lett.*, vol. 32, no. 8, pp. 1083–1085, Aug. 2011, doi: 10.1109/LED.2011.2158057.

[28] Y. Liu *et al.*, "Low-frequency noise in hydrogenated amorphous silicon thin film transistor," *Acta Physica Sinica*, vol. 66, no. 23, Dec. 2017, Art. no. 237101, doi: 10.7498/aps.66.237101.

[29] N. V. Duy *et al.*, "Effect of series resistance on field-effect mobility at varying channel lengths and investigation into the enhancement of source/drain metallized thin-film transistor characteristics," *Jpn. J. Appl. Phys.*, vol. 50, no. 2, Feb. 2011, Art. no. 024101, doi: 10.1143/JJAP.50.024101.

[30] A. Tsormpatzoglou, N. A. Hastas, S. Khan, M. Hatalis, and C. A. Dimitriadis, "Comparative study of active-over-metal and metal-over-active amorphous IGZO thin-film transistors with low-frequency noise measurements," *IEEE Electron Device Lett.*, vol. 33, no. 4, pp. 555–557, Apr. 2012, doi: 10.1109/LED.2012.2185677.

[31] C. A. Dimitriadis, F. V. Farmakis, G. Kamarinos, and J. Brini, "Origin of low-frequency noise in polycrystalline silicon thin-film transistors," *J. Appl. Phys.*, vol. 91, no. 12, pp. 9919–9923, Jun. 2002, doi: 10.1063/1.1481964.

[32] J. Lee *et al.*, "Fully transfer characteristic-based technique for surface potential and subgap density of states in p-channel polymer-based TFTs," *IEEE Electron Device Lett.*, vol. 34, no. 12, pp. 1521–1523, Dec. 2013, doi: 10.1109/LED.2013.2280014.

[33] L. Pichon, A. Boukhenoufa, C. Cordier, and B. Cretu, "Determination of interface state distribution in polysilicon thin film transistors from low-frequency noise measurements: Application to analysis of electrical properties," *J. Appl. Phys.*, vol. 100, no. 5, Sep. 2006, Art. no. 054504, doi: 10.1063/1.2335395.

[34] L. Pichon, B. Cretu, and A. Boukhenoufa, "Thermal dependence of low-frequency noise in polysilicon thin film transistors," *Thin Soild Films*, vol. 517, no. 23, pp. 6367–6370, Oct. 2009, doi: 10.1016/j.tsf.2009.02.055.

[35] M. Shur and M. Hack, "Physics of amorphous silicon based alloy field-effect transistors," *J. Appl. Phys.*, vol. 55, no. 10, pp. 3831–3842, May 1984, doi: 10.1063/1.332893.

[36] Y. Liu, R.-H. Yao, B. Li, and W.-L. Deng, "An analytical model based on surface potential for a-Si:H thin-film transistors," *J. Display Technol.*, vol. 4, no. 2, pp. 180–187, Jun. 2008, doi: 10.1109/JDT.2007.907122.

[37] J. C. Park *et al.*, "Low-frequency noise in amorphous indium-gallium-zinc oxide thin-film transistors from subthreshold to saturation," *Appl. Phys. Lett.*, vol. 97, no. 12, Sep. 2010, Art. no. 122104, doi: 10.1063/1.3491553.

[38] G. Reimbold, "Modified 1/f trapping noise theory and experiments in MOS transistors biased from weak to strong inversion—Influence of interface states," *IEEE Trans. Electron Devices*, vol. 31, no. 9, pp. 1190–1198, Sep. 1984, doi: 10.1109/T-ED.1984.21687.

YUAN LIU (S'07–M'09) received the B.S. and Ph.D. degrees in electrical engineering from the South China University of Technology, Guangzhou, China, in 2004 and 2009, respectively.

From 2011 to 2017, he was a Senior Engineer with the China Electronic Product Reliability and Environmental Testing Research Institute. Since 2018, he has been an Associate Professor with the School of Microelectronics, South China University of Technology. His research interests include characterization, modeling, and reliability of semiconductor devices.

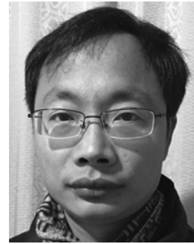

HONGYU HE (M'16) received the B.S. degree in electronic science and technology and the M.S. degree in microelectronics and solid-state electronics from the Huazhong University of Science and Technology, Wuhan, China, in 2001 and 2004, respectively, and the Ph.D. degree in microelectronics and solid-state electronics from the South China University of Technology, Guangzhou, China, in 2011.

Since 2016, he has been an Associate Professor with the School of Electrical Engineering, University of South China, Hengyang, China. His research interests include characterization and modeling of thin film transistors.

RONGSHENG CHEN (M'16) received the Ph.D. degree from the Department of Electronic and Computer Engineering, Hong Kong University of Science and Technology, Hong Kong, in 2013.

He is currently an Associate Professor with the School of Microelectronics, South China University of Technology, Guangzhou. His current research interests include low temperature poly-Si thin-film transistors (TFTs), metal oxide TFTs, and their application in active matrix displays.

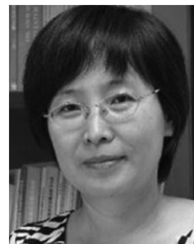

YUN-FEI EN (M'09) received the B.S., M.S., and Ph.D. degrees in microelectronics from Xidian University, Xi'an, China, in 1990, 1995, and 2013, respectively.

She is currently a Professor with the China Electronic Product Reliability and Environmental Testing Research Institute. Her current research interests include characterization and failure analysis of electronic components.

BIN LI (M'02) received the B.S. and M.S. degrees in electrical engineering from the South China University of Technology, Guangzhou, China, in 1989 and 1992, respectively, and the Ph.D. degree in electrical engineering from the University of Hong Kong, Hong Kong, in 2001.

She is currently a Professor with the School of Microelectronics, South China University of Technology. Her current research interests include device physics and circuit design.

YI-QIANG CHEN (M'11) received the B.S. degree in microelectronics and the Ph.D. degree in material science and engineer from Xiangtan University in 2006 and 2011, respectively.

In 2011, he joined the China Electronic Product Reliability and Environmental Testing Research Institute and is currently a Senior Research Engineer. His research interests include reliability mechanism and modeling of microelectronics devices and power devices on the base of wide band semiconductor.